Supporting Information

Liu et al. 10.1073/pnas.1419312112

SI Text

Surface Properties. The addition of fluorinated monomer compound **4** to the mixture changes the surface properties. This fluorinated monomer, besides its function as nucleation agent for domain formation, also reduces the surface tension of the films as a result of its surfactant-like property. This, for instance, manifests itself by an increase in contact angle of a water droplet from 70° to 115° bringing the concentration of the fluorinated compound from zero (Fig. S1*A*) to 1.5 wt % (Fig. S1*B*). The surface being enriched with these fluorinated groups also reduces the friction of the coating. The kinetic friction coefficient is measured in a home-built system (1) by sliding two LCN surfaces against each other with a sliding speed of 0.1 mm·s^{-1}. The measured force is plotted versus the load on the surfaces (Fig. S1*C*). The tangent of this linear function gives kinetic friction coefficient (μ_k) following Amontons' first law of friction written as $\mu_k = F_f/F_N$. The friction coefficient of the compound **4** modified sample is measured to be considerably lower ($\mu_k = 0.08$) than that of a reference sample without the fluorinated monomer ($\mu_k = 0.5$).

Kinetic Measurements. An important aspect of the formation of the surface structures is the kinetics with which they are formed. We analyzed that with two methods. In the first method we analyzed the change of positions of a surface element by transient interference measurements using a reflection configured digital holographic microscope (Lyncee Tec). Fig. S2 shows a typical example of the relative height change of an arbitrary surface element. After switching on the light-emitting diode (LED) lamp (365 nm) 80% of the maximum height is reached within 10 s. Switching off the lamp gives a fast relaxation to around 50% of the maximum height within 1 s, after which a slower relaxation process starts to come to the initial flat surface. According to Fig. S2 it takes about 10 s for the structures to reach a value of 20% of the maximum height.

The second method is based on measuring the transient kinetic friction coefficient while the LED lamp is switched on and off. The friction force is proportional to the normal loading (Fig. S1*A*). This means that the kinetic friction coefficient (μ_k) is a constant, independent of loading force and the sliding velocity as long as the surface structure does not deform under the load. In the flat state, without UV activation, μ_k is on the order of 0.08; activation by UV exposure revealed that μ_k increased to 0.3 (Fig. S3*A*). Fig. S1*B* shows the change in friction force F_f when the coating is switched from the flat state to the corrugated by starting the illumination while the samples are shifting along each other with a weight of 0.5 N. The increased friction is attributed to the formation of interlocking surface topographies. This observation contradicts earlier observations of more regular structures of constant height that reduce their μ_k. Here interlocking was prevented and the coatings were sliding on the tops of the structures; the decrease in μ_k relates to the smaller contact area. In the case of the polydomain coating the surface roughness is much more irregular and two structures brought in contact will "sink" into one another. The time that it takes to reach the maximum friction after switching on the UV source is around 5 s. After switching off the UV light the original friction force of the flat coatings is retrieved within 10 s as the spikes are erased.

Fitting of the Light Penetration Parameters. To validate the experimental results in terms of the assumed mechanistic model, we simulated the polydomain structure using the methodology provided in *Materials and Methods*. Necessary input parameters are the dimensionless numbers α and β, the order parameter of the liquid crystal network S, the quantum efficiency ratio η, and the attenuation length for the *trans* state d_t. The source light is diffuse and propagates normal to the top surface. The order parameter S is taken to be 0.7, a typical value for glassy liquid crystal polymers (2). For the ratio of quantum efficiencies η we use an estimated value of 3 from ref. 3. Now one can calculate α, β, and d_t by comparing the calculated and measured transmitted light intensity for different source intensities. The experiments were done for a sample with a thickness of 7.7 μm, 5 wt % azobenzene, and various incoming intensities. The best-fitted model parameters were found to be $\alpha = 54.9$, $\beta = 14.3$ for the illumination intensity of 600 mW·cm^{-2}, and the attenuation length $d_t = 0.998$ μm. Details on the fitting procedure can be found in Fig. S4 and Table S1.

Definition of Axes and Director Angle. Various structures were constructed with a thickness of 5 μm and an in-plane domain size ranging from 2.5 to 20 μm. For each domain the director orientation is randomly chosen by picking the tilt angle ϕ and the azimuth angle θ from a uniform distribution between 0 and 180° and between 0 and 360°, respectively (Fig. S5).

Surface Profiles as Function of Domain Size. In the main text, the 3D surface corrugation profile superimposed by a contour plot for the displacement along the thickness direction u_z (in μm) for domain sizes of 5 and 15 μm is shown in Fig. 6 *C* and *E*, respectively. Here the influence of the domain size is worked out further. Results for domain sizes of 2.5, 10, and 20 μm are presented in Figs. S6, S7, and S8, respectively.

Influence of Domain Aspect Ratios and Film Thickness on the Actuated Surface Roughness. Coatings with small domain sizes were found to generate protrusions that are rougher and spikier compared with the coatings with larger domain sizes. In Figs. S9 and S10 we present the effect of the modeled aspect ratios for a fixed film thickness (equal to 5 d_t). The reason for the decreased depth modulation with decreasing domain size is related to the increased level of constraint that the domains impose on each other. Another manifestation of the mechanical constraints was found to be present in situations where planar domains were surrounded by domains with directors close to homeotropic, leading to an enhancement of the planar domain's surface expansion.

We carried out additional simulations to study the effect of film thickness (normalized by the attenuation length d_t) on the Wenzel roughness for a fixed aspect ratio (equal to 3). These results are shown in Fig. S11. The results show a strong (close to linear) dependence of the depth modulation and a weak dependence of the roughness on the film thickness, as expected from dimensional arguments.

Preservation of *trans* State of Azobenzene During Photopolymerization. The azobenzene moieties are known to be converted from their *trans* state to the *cis* state by exposure to UV light. During the formation of the film by photopolymerization this should be prevented as it already will reduce the order of the polymer film before the actuation experiments. For this reason photopolymerization is carried out by light >400 nm using a cutoff filter (*Materials and Methods*). To check whether this was sufficient a UV-VIS spectrum of the sample is taken after the polymerization process but before the actuation experiments (Fig. S12). The measurement demonstrates that the azobenzene kept its *trans* state.

1. Liu D, Broer DJ (2014) Self-assembled dynamic 3D fingerprints in liquid-crystal coatings towards controllable friction and adhesion. *Angew Chem Int Ed Engl* 53(18):4542–4546.
2. Heynderickx I, Broer DJ, Van Den Boom H, Teesselink WJD (1992) Liquid-crystalline ordering in polymeric networks as studied by polarized raman scattering. *Journal of Polymer Science Part B* 30(2):215–220.
3. Gadelmawla ES, Koura MM, Maksoud TMA, Elewa IM, Soliman HH (2002) Roughness parameters. *J Mater Process Technol* 123(1):133–145.

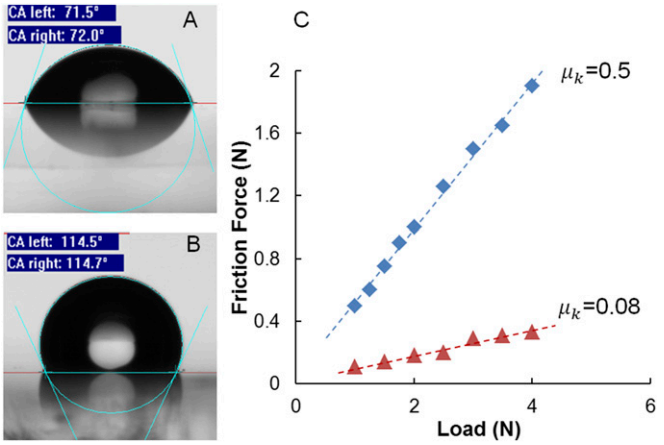

Fig. S1. Comparison of the flat liquid crystal coating in terms of contact angle (CA) of a water droplet between (*A*) a liquid crystal (LC) surface without the presence of **4** and (*B*) coating modified with **4**. (*C*) The kinetic friction coefficient (μ_k) of the LC surface free of **4** (blue squares) and with **4** (red triangles).

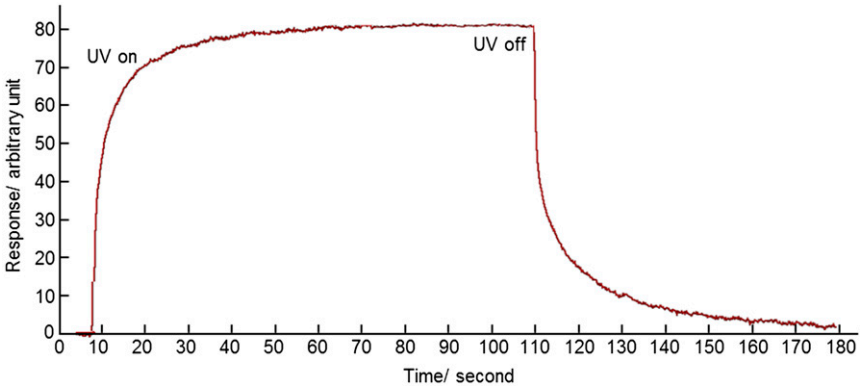

Fig. S2. Dynamics of the surface topographies are measured by time-resolved interference microscopy.

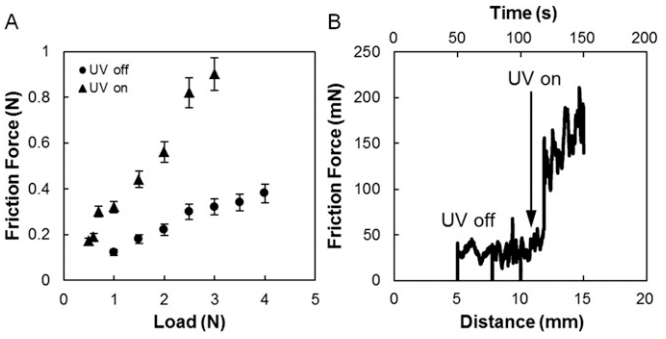

Fig. S3. Dynamics of the friction. (*A*) Friction forces versus loading. (*B*) Dynamic force traces when the surface topographies are switched from the "off" to the "on" state. The normal loading exerted on the two coatings is 0.5 N.

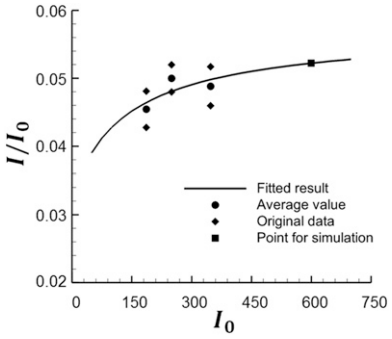

Fig. S4. Fitting of the light penetration parameters α, β, and d_t. Diamond symbols are original measured reduced transmitted intensities over the source intensities. Circles are the corresponding average values. The curve is obtained by following the least-squares fitting method against the average values. The final input for our finite element model consists of $\alpha = 54.9$ and $\beta = 14.3$ for the illumination intensity of 600 mW·cm^{-2}and the attenuation length $d_t = 0.998$ μm.

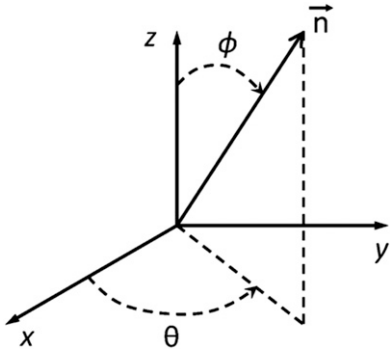

Fig. S5. Orientation of the director: the tilt angle ϕ is the angle between the director $\vec{n}$ and the z axis, and the azimuth angle θ is the angle between the x axis and the projection of $\vec{n}$ in the x–y plane. The ϕ ranges from 0 to 180° and θ from 0 to 360°.

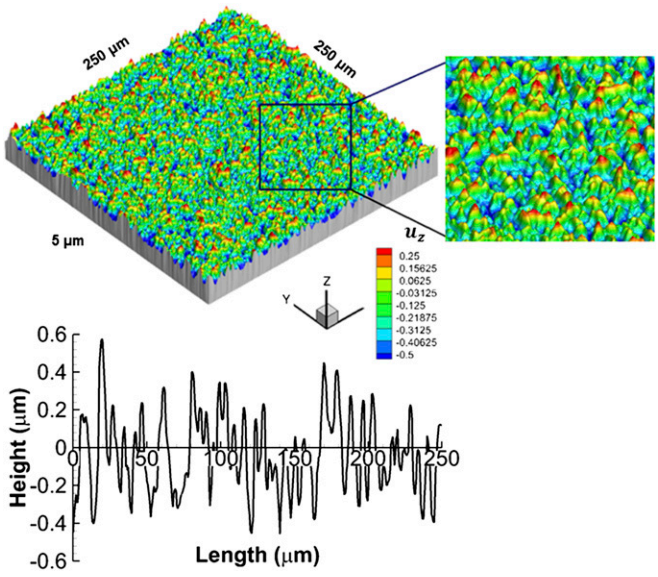

Fig. S6. Predicted 3D surface reliefs with a contour plot for the displacement along the thickness direction u_z (in micrometers) and a corresponding surface profile relative to the average activated surface height of the LC coating. A partial enlargement of the surface is shown as well. The domain size is equal to 2.5 μm, corresponding to an aspect ratio (domain size over film thickness) of 0.5.

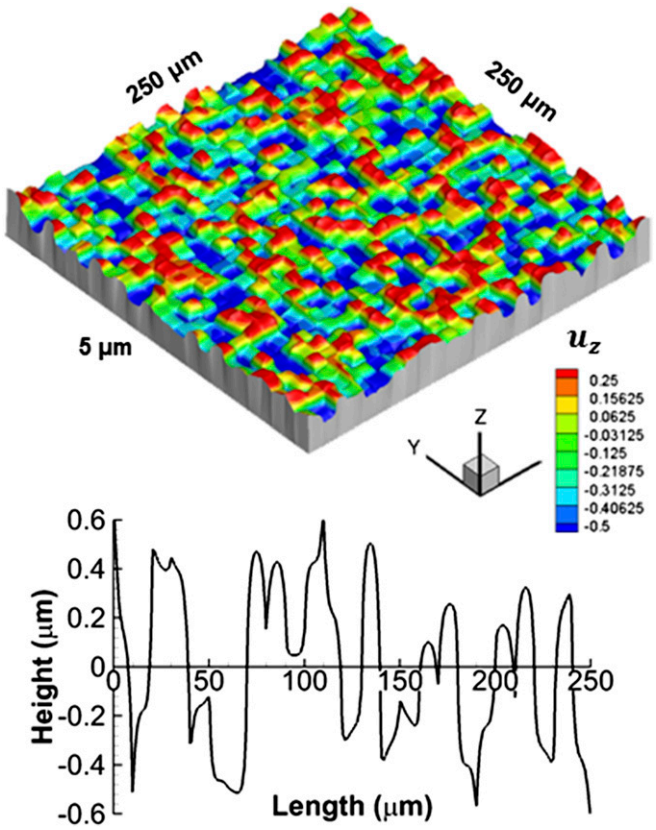

Fig. S7. Predicted 3D surface reliefs with a contour plot for the displacement along the thickness direction u_z (in micrometers) and a corresponding surface profile relative to the average activated surface height of the LC coating. The domain size is equal to 10 μm, corresponding to an aspect ratio (domain size over film thickness) of 2.

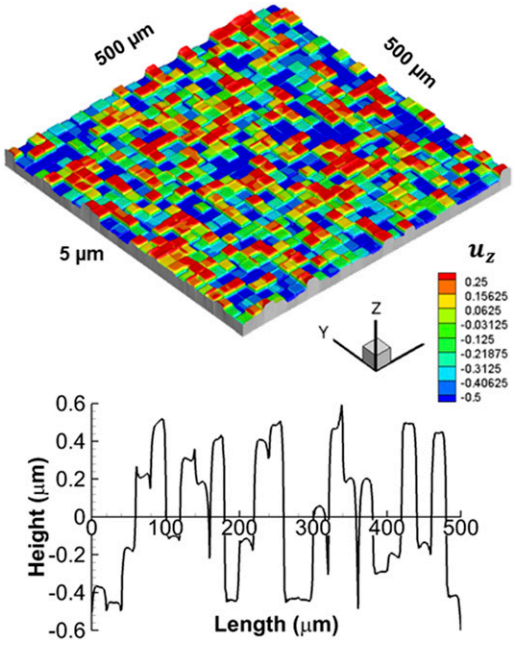

Fig. S8. Predicted 3D surface reliefs with a contour plot for the displacement along the thickness direction u_z (in micrometers) and a corresponding surface profile relative to the average activated surface height of the LC coating. The domain size is equal to 20 μm, corresponding to an aspect ratio (domain size over film thickness) of 4.

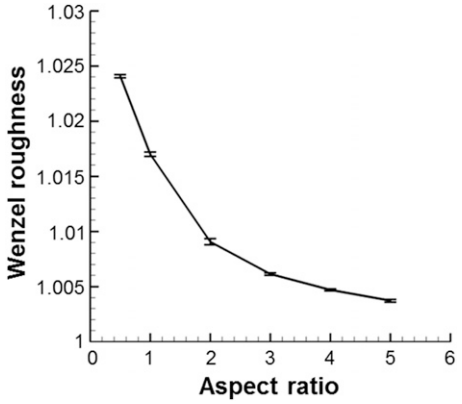

Fig. S9. Predicted variation of the Wenzel roughness parameter as a function of aspect ratio (domain size divided by film thickness) for a film thickness of $5d_t$. The Wenzel roughness parameter is defined as the ratio between the real area of the surface and the projected area onto the x–y plane.

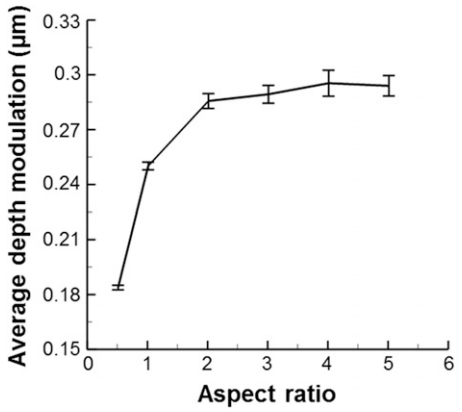

Fig. S10. Predicted variation of the average depth modulation (3) as a function of aspect ratio (domain size divided by film thickness) for a film thickness of $5d_t$.

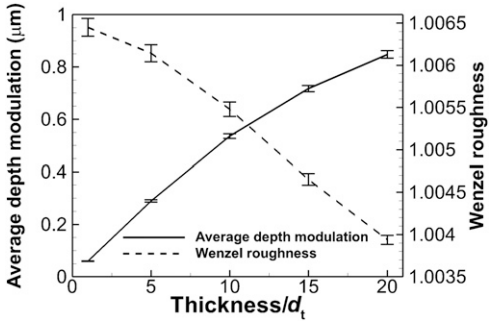

Fig. S11. The variation of the average depth modulation (3) and the Wenzel roughness parameter as a function of film thickness (normalized by d_t) for an aspect ratio (domain size divided by film thickness) equal to 3.

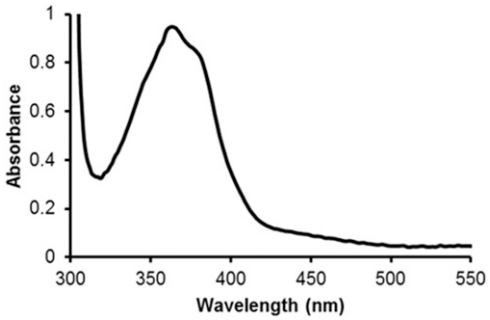

Fig. S12. Absorption spectrum of polydomain film measured after polymerization with the characteristic absorption band of the azobenzene group, demonstrating that the azobenzene is not converted to the *cis* state by the photopolymerization process.

Table S1. Transmittance measurement for a planar LC coating under diffuse light illumination normal to the coating having a thickness of 7.7 μm

Source light intensity, mW·cm^{-2}	Transmitted intensity, mW·cm^{-2}
348	16–18
250	12–13
187	8–9